

Dinitrosyl formation as an intermediate stage of the reduction of NO in the presence of MoO_3

Ioannis N. Remediakis* and Efthimios Kaxiras

Department of Physics and Division of Engineering and Applied Sciences, Harvard University, Cambridge MA 02138*

Melvin Chen and Cynthia M. Friend

Department of Chemistry, Harvard University, Cambridge MA 02138

(Dated: November 4, 2018)

We present first-principles calculations in the framework of density-functional theory and the pseudopotential approach, aiming to model the intermediate stages of the reduction of NO in the presence of $\text{MoO}_3(010)$. In particular, we study the formation of dinitrosyl, which proves to be an important intermediate stage in the catalytic reduction. We find that the replacement of an oxygen of MoO_3 by NO is energetically favorable, and that the system lowers further its energy by the formation of $(\text{NO})_2$. Moreover, the geometry and charge distribution for the adsorbed dinitrosyl indicates a metal-oxide mediated coupling between the two nitrogen and the two oxygen atoms. We discuss the mechanisms for the dinitrosyl formation and the role of the oxide in the reaction.

[To be published in the Journal of Chemical Physics]

Reduction of nitric oxide (NO) has long been the focus of detailed studies, because of the role of NO as pollutant in the atmosphere. Three-way catalysts, based on Rh, Pt or PdO are used in automobile exhausts for this purpose; the effectiveness of such catalysts was found to increase when molybdenum oxides are added^{1,2}. Recently, it was proposed that the NO reduction products N_2 and O_2 are formed nondissociatively from NO via an adsorbed dinitrosyl species, which facilitates N-N coupling³, since low temperature NO coupling proceeds through a dinitrosyl intermediate⁴. The geometry of the adsorbed dinitrosyl and the mechanism of N-N coupling remain unknown. To address this important question, we perform first-principles calculations based on density-functional theory and the pseudopotential approach, for various configurations involving nitrosyls and the $\text{MoO}_3(010)$ surface. The paper is organized as follows: First, we review the structure of MoO_3 and describe the method we use for the calculations. Next, we present our results for the $\text{MoO}_3(010)$ surface with an O vacancy, a structure with an exposed Mo atom which can adsorb NO molecules. This is followed by detailed analysis of the configurations involving adsorbed NO and $(\text{NO})_2$. Finally, we discuss the dinitrosyl formation mechanisms and the role of the $\text{MoO}_3(010)$ surface as a catalyst for the reduction of NO.

I. MOLYBDENUM TRIOXIDE

Molybdenum trioxide is a layered material, its layers being weakly bonded via van der Waals interactions. The space group is Q_h^{16} (bnm), and the lattice is orthorhombic⁵ with parameters⁶ 3.962, 13.858,

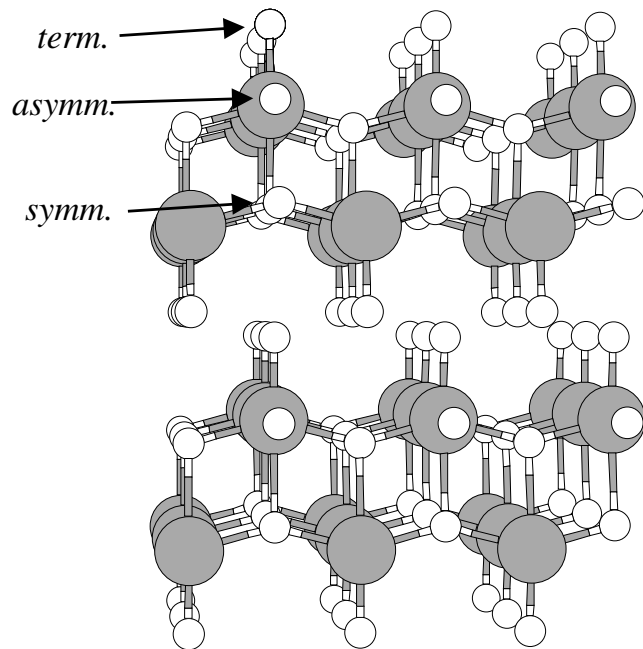


FIG. 1: Structure of bulk MoO_3 . Mo atoms are shown as larger gray spheres, O atoms as white, smaller spheres. The three different types of O atoms (terminal, asymmetric bridging, symmetric bridging) are indicated.

and 3.697 Å. Each unit cell contains four MoO_3 units. The lattice coordinates of the atoms are $\pm(x, y, \frac{1}{4})$ and $\pm(\frac{1}{2} - x, \frac{1}{2} + y, \frac{1}{4})$, with (x, y) equal to (0.086, 0.099) for the Mo atoms, and (0.086, 0.250), (0.586, 0.099), (0.586, 0.431) for the three O atoms surrounding each Mo atom, respectively⁶.

The MoO_3 crystal is shown in Fig. 1. Macroscopically, the material forms “small, thin, lustrous plates, parallel to (010)”⁵. This is revealed in the atomistic structure: It consists of bilayers parallel to the (010) plane, which are bonded through weak electrostatic interactions, with

*Present address: Center for Atomic-scale Materials Physics, Department of Physics, Building 307, Technical University of Denmark, 2800 Lyngby, Denmark

the (010) surface being the easy cleavage plane of the crystal. Each bilayer consists of two sublayers of periodically arranged distorted MoO_6 octahedra. There are three structurally different O atoms. The *asymmetric bridging* oxygen is collinear with two Mo atoms and forms one long and one short bond with them. The *symmetric bridging* oxygen is located between the two sublayers of the bilayer and bonds to two Mo atoms of one sublayer with equal bond lengths and to one Mo atom of the other sublayer with an elongated bond. Finally, the univalent *terminal* oxygen is connected to one Mo atom forming the shortest Mo-O bond in the system. The Mo-O bond lengths in MoO_3 as obtained from several experimental and theoretical studies are shown in Table I.

II. THE CALCULATION

All calculations reported in this work were performed via the High-performance-Fortran Adaptive Real-space Electronic Structure (HARES) package¹⁰. We use Density-Functional Theory (DFT) in the Local Spin Density Approximation (LSDA)^{11,12}. The Kohn-Sham valence electron wavefunctions are represented in a real-space orthogonal grid with a spacing of 0.13 Å, which is equivalent to a cut-off energy of 150 Ry in a plane-wave basis calculation. The ionic cores and their interaction with valence electrons were taken into account through the soft Troullier-Martins¹³ pseudopotentials, in the separable Kleinman-Bylander form¹⁴. The Laplacian is expanded to second order terms. For the exchange-correlation functional we use the results of Ceperley and Alder as parametrized by Perdew and Zunger¹⁵. The electronic density was updated during the self-consistent loop using a modified Broyden mixer¹⁶.

We model the surface of MoO_3 by a single bilayer perpendicular to the (010) direction. This approximation is not expected to affect the results, due to the weak inter-layer coupling. The calculated Mo-O bond lengths for the single-bilayer system are shown in Table I. As experimental data have discrepancies, we compare our results to the average of the two sets (last column of Table I). The agreement to experiment is within 2%. Our results are also in agreement to the calculation of Yin *et al.*⁸. Moreover, vibrational frequencies calculated within the single bilayer approximation⁷ are also in very good agreement with experiment. This justifies our choice to use a simplified unit cell, while establishing the adequacy of DFT and HARES to correctly describe bonding in the material under study. The surface unit cell we chose has (2×2) periodicity relative to the ideal structure. This is sufficient to simulate isolated O vacancies or adsorbed NO, due to the local character of the substrate-adsorbate interaction and the lack of reconstruction effects for this surface. The Brillouin Zone was sampled by the Γ point only, which is adequate due to the large size of the unit cell. The atomic degrees of freedom were relaxed with the Broyden-Fletcher-

Goldfarb-Shanno (BFGS) method^{17,18} until the calculated Hellman-Feynman forces were smaller in magnitude than 0.005 a.u. We used the symmetry of the problem to eliminate some electronic as well as ionic degrees of freedom where appropriate (see below). We have checked these computational parameters against previous calculations^{10,19} of similar systems to make sure they give well-converged results.

III. TERMINAL O VACANCY AND NO ADSORPTION

An O vacancy in MoO_3 is formed when a terminal oxygen atom is missing. As discussed in Section I, the terminal O is univalent and forms the shortest Mo-O bond in the bulk; this bond is also the strongest, with a calculated²⁰ bond order of 1.93. Accordingly, it is expected that the formation energy of the vacancy will be high. Indeed, our calculation yields a formation energy of 2.95 eV/vacancy, assuming that the O atoms that leave the surface form O_2 molecules (see Table III). The (2×2) unit cell corresponds to a 0.25 ML coverage of vacancies, which is low enough to ensure that the interactions between vacancies are negligible. The formation of the O vacancy is accompanied by small relaxations of atoms around the missing terminal O atom. The relaxed geometry is shown in Fig. 2(a). The main effect is an inward displacement of the exposed Mo atom, which results in shrinking the Mo-symmetric oxygen bonds from 1.96 Å to 1.91 Å for O in the same sublayer and from 2.33 Å to 2.11 Å for O in the adjacent sublayer. None of the atoms has any significant displacement parallel to the (010) plane; we thus find no evidence of surface reconstruction due to vacancy formation.

The $\text{MoO}_3(010)$ surface with a terminal oxygen vacancy, shown in Fig. 2(a), has many characteristics of a good catalytic platform: The exposed Mo atom promises to be chemically active and has the ability to bond to more than one adsorbate atoms, since it has lost a double bond. The remaining terminal O atoms around the vacancy site form a cage structure that can enhance coupling between the adsorbates. In ideal MoO_3 , the calculated²⁰ population for a terminal O is -0.4 electrons, so the remaining terminal O atoms are expected to repel the adsorbates, creating an implicit attraction between them.

The first step in the catalytic reduction of NO is the adsorption of a NO molecule. The binding configuration is shown in Fig. 2(b). NO is bonded to a Mo atom and substitutes a terminal O. The molecule is perpendicular to the surface in the lowest energy geometry, rendering the dissociation of nitrosyl on the surface implausible. The adsorption of NO on MoO_3 with an O vacancy restores the positions of the surrounding atoms to their positions in the ideal $\text{MoO}_3(010)$ surface: the lengths of the Mo-N and N-O bonds are 1.91 and 1.14 Å, respectively. The N-O bond has very similar length to the bond

TABLE I: Bond lengths (in Å) between Mo and O in MoO_3 as calculated in the present work compared to other calculations (a) by Chen *et al.*⁷ and (b) by Yin *et al.*⁸ and to experimental data obtained from (c) the atomic positions given by Wyckoff⁶ and (d) the work of Kihlborg⁹ as given in Ref.⁷. The symbols O_t , O_s and O_a denote the terminal, symmetric bridging and asymmetric bridging O atoms respectively.

Bond	Bond Length					
	This work	Theory (a)	Theory (b)	Exp. (c)	Exp. (d)	Exp. (avg)
Mo- O_t	1.77	1.67	1.76	1.82	1.67	1.75
Mo- O_s	1.96	1.92	2.02	1.93	1.95	1.94
	2.33	2.30	2.28	2.32	2.33	2.33
Mo- O_t	1.87	1.76	1.81	1.89	1.73	1.81
	2.17	2.19	2.25	2.08	2.25	2.17

of a free NO molecule. We find this bond to be 1.15 Å, in excellent agreement to experiment.

The binding energy for NO to the $\text{MoO}_3(010)$ surface with an oxygen vacancy is 2.98 eV/molecule. The energy difference between the $\text{MoO}_3(010)$ surface and the same surface with NO substituting a terminal O is -0.03 eV/molecule, assuming that the O atoms leaving the surface form O_2 molecules. The system lowers its total energy by the substitution of terminal O by NO, so this configuration must be an important step in the NO reduction. The mechanism of the substitution and the formation of O_2 gas is not known, but it seems unlikely that the system passes through the O vacancy configuration, since the barrier for this path would be at least 2.95 eV, a number which would forbid the process under ordinary conditions. The transition state for the substitution could involve intermediate formation of NO_2 and/or O_3 .

NO adsorption could also take place after a vacancy on the surface has been formed by an independent mechanism, for example after a CO molecule has hit the surface and CO_2 has been formed. Another similar mechanism would be the formation of H_2O from gas-phase H_2 and a terminal O atom. The exact final product of the reduction of $\text{MoO}_3(010)$ to $\text{MoO}_3[\text{v}](010)$ cannot be *ad hoc* determined, as it depends on the experimental conditions. However, the final state of the O atom that leaves the surface to create the vacancy would not affect the picture, as the energetics would not change dramatically. We therefore choose to use O_2 as a typical product of a reduction reaction.

IV. DINITROSYL CHEMISORPTION

To study the energetics of the dinitrosyl adsorption, we consider two characteristic configurations: In the first, the $(\text{NO})_2$ plane is parallel to (001) or the plane defined by the Mo atom and the symmetric bridging O atoms. In the second configuration, the $(\text{NO})_2$ plane is parallel to (100), or a plane perpendicular to the previous one which contains the Mo atom and the asymmetric bridging O atoms. The relaxed geometries for both configurations

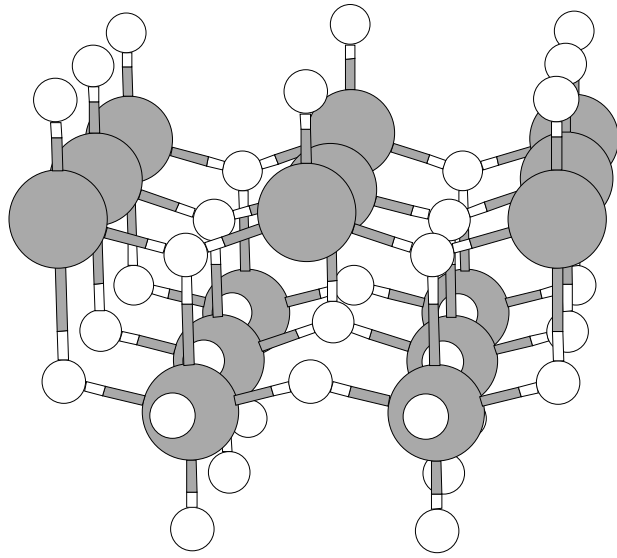
TABLE II: Bond lengths (in Å) for the various structures discussed in the text. O_t , O_s and O_a stands for the terminal, symmetric bridging and asymmetric bridging O, respectively. The Mo- O_s bonds for Mo and O_s belonging at the same or adjacent sublayers, as well as the short and long Mo- O_a bond are shown. (s) and (a) indexes for adsorbed $(\text{NO})_2$ refer to adsorption with the molecule parallel to the symmetric and asymmetric bridging O planes, respectively.

Structure	Mo - O_t	Mo- O_s		Mo- O_a		Mo-N	N-O	N-N
		same	adj.	short	long			
Ideal	1.77	1.96	2.33	1.87	2.17	-	-	-
O vacancy	1.77	1.91	2.11	1.90	2.06	-	-	-
ads. NO	1.77	1.95	2.23	1.86	2.15	1.91	1.14	-
ads. $(\text{NO})_2$ (s)	1.78	1.98	2.36	1.89	2.16	2.00	1.14	2.18
ads. $(\text{NO})_2$ (a)	1.78	1.96	2.29	1.90	2.18	1.95	1.15	2.21
						2.35	1.13	

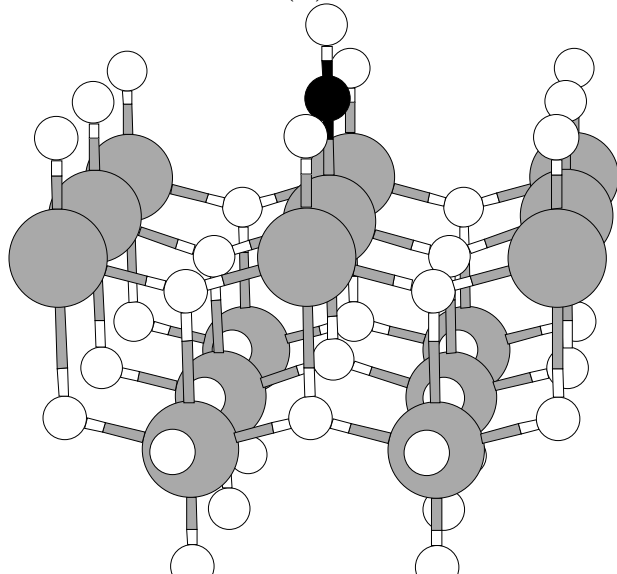
are shown in Fig. 3.

In the first case, a reflection symmetry with respect to the (100) plane was imposed, following the experimental results obtained on oxidized $\text{Mo}(110)^3$. Removal of the reflection symmetry does not result in further relaxation or significant lowering of the total energy, indicating that in the lowest energy geometry the two NO molecules of the dinitrosyl are identical. By contrast, $(\text{NO})_2$ adsorbed parallel to the (100) plane is found to be strongly asymmetric, with one of the two NO molecules closer to the Mo center than the other. This is a direct consequence of the asymmetry of the underlying oxygen atoms.

The bond lengths for both configurations, together with the bond lengths of the previously discussed structures are summarized in Table II. For adsorbed dinitrosyl in the Mo-symmetric O plane, the Mo-N bond is 2.00 Å long, 5% longer than in that of a single adsorbed NO. The Mo-N bond is weaker for adsorbed $(\text{NO})_2$ as the bonding electrons of Mo are shared by two N atoms. The N-O bond length is 1.14 Å, identical to that of adsorbed NO. In the second configuration, having dinitrosyl



(a)

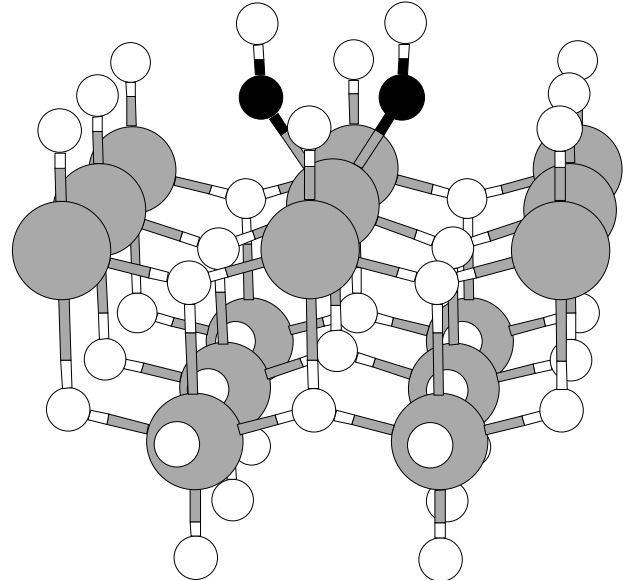


(b)

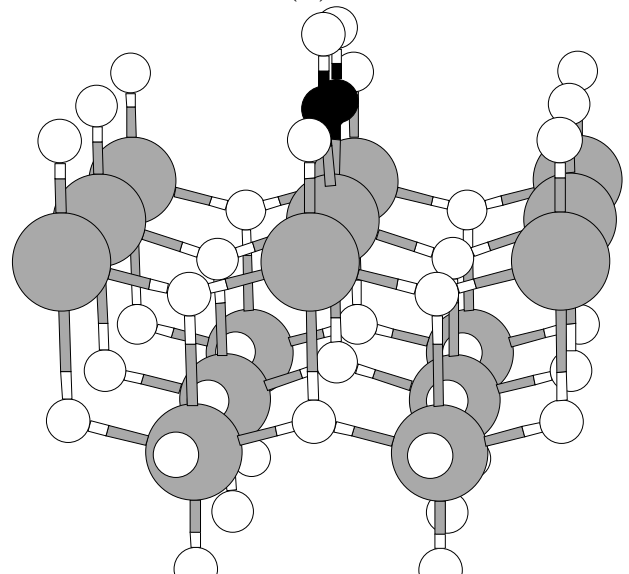
FIG. 2: Relaxed geometries for $\text{MoO}_3(010)$ (a) with a terminal O vacancy and (b) with an adsorbed NO molecule. Grey, white and black spheres correspond to Mo, O and N atoms, respectively.

in the Mo-asymmetric O plane, the Mo-N (N-O) bonds have lengths 1.95(1.15) and 2.35(1.13) Å, for NO above the long (2.18 Å) and short (1.90 Å) Mo-asymmetric O bond, respectively. Both N and O of the adsorbed nitrosyls are more strongly bound above the less strongly bonded asymmetric O.

The asymmetric configuration, with $(\text{NO})_2$ parallel to the Mo-asymmetric O plane, has a slightly lower energy than the other, by 0.10 eV per $(\text{NO})_2$ molecule. The binding energy to $\text{MoO}_3(010)$ with an oxygen vacancy is 3.80 eV and 3.90 eV per molecule for the symmetric and



(a)



(b)

FIG. 3: Relaxed geometries for dinitrosyl adsorption (a) in the symmetric O plane and (b) in the asymmetric O plane.

asymmetric configuration, respectively. The energy gain when $(\text{NO})_2$ substitutes a terminal O of $\text{MoO}_3(010)$ with formation of O_2 gas is 0.85 eV and 0.95 eV per molecule for the two configurations.

The large lowering of the total energy by 0.90 eV on average per molecule for $(\text{NO})_2$ adsorption, compared to 0.03 eV per NO for the NO adsorption, indicates that bonding between the two parts of the dinitrosyl has taken place. This bonding is evident in Fig. 4, which presents a contour plot of the total electronic density minus a superposition of atomic electronic densities on the dinitrosyl plane, which coincides with the symmetric bridging O plane. According to our choice of shading, electronic

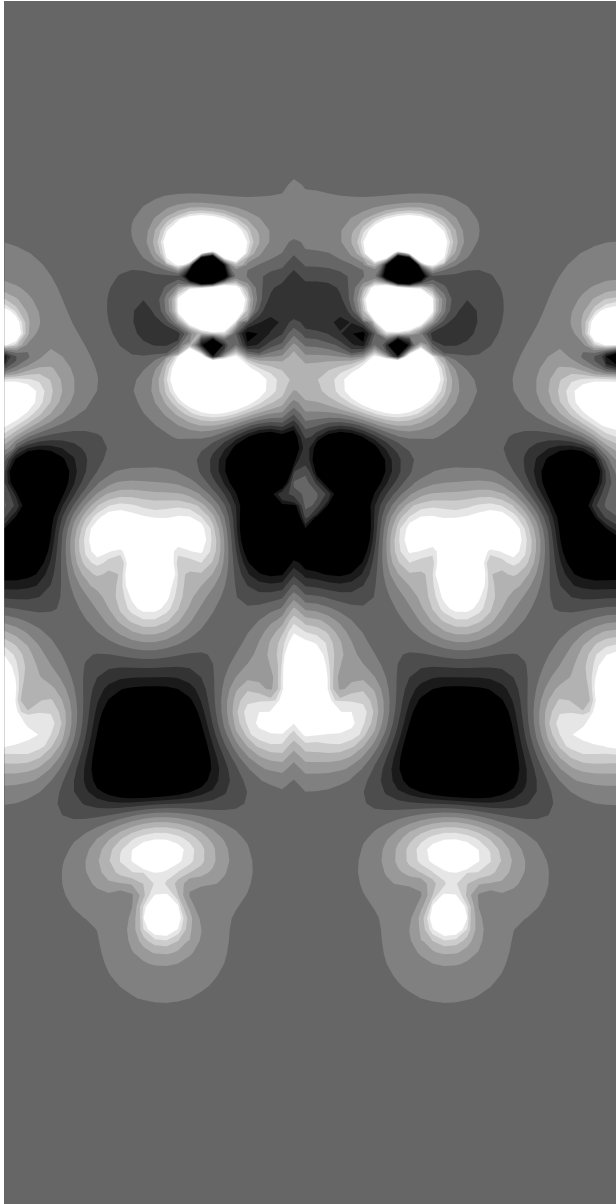


FIG. 4: Contour plot of total electronic density minus a superposition of valence atomic charge densities in the Mo-N-O plane for adsorbed $(NO)_2$ parallel to the symmetric O plane. The background shade corresponds to zero; darker shades correspond to negative values, lighter shades to positive values.

charge has moved from the darker to the lighter regions, relative to the charge distribution of a superposition of atomic densities. The white T-shaped clouds inside the slab correspond to symmetric bridging O atoms, while those at the bottom to terminal O atoms. Small gray spots in the middle of black regions correspond to Mo atoms. The two bright vertical complexes correspond to the two NO molecules. As the electronegativities of the involved elements dictate, charge has moved from the Mo atoms to N and O atoms, with O atoms having slightly

more charge concentrated around them compared to N atoms.

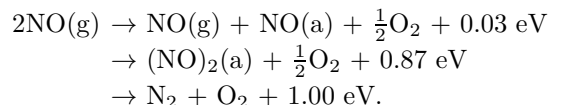
We observe an apparent electron sharing between the two N atoms, manifesting the N-N coupling due to the presence of the catalytic surface. A similar, but weaker, coupling exists between the O atoms of the dinitrosyl. The absence of bonding charge between the N atoms of the adsorbate and the surrounding terminal O atoms implies a repulsion between them. It is this repulsion that leads to the attraction between the N atoms.

V. DISCUSSION

The reactions leading to dinitrosyl formation, starting either with gas phase NO or with adsorbed nitrosyl, are summarized in Table III. Although the adsorption of two gas NO molecules to form a dinitrosyl is exothermic by 0.90 eV/molecule (this number is the average between the two characteristic geometries of the dinitrosyl discussed before), the process is expected to have a large energy barrier due to the repulsion of the NO molecules, which, having an electrical dipole moment, would prefer to have an anti-parallel configuration. The combination of two adsorbed nitrosyls is also rejected as a mechanism for dinitrosyl formation, as the vacancy left behind makes the process energetically costly. Indeed, as shown in Table III, this reaction is endothermic by more than 2 eV/molecule. The alternative is to fill the O vacancy by an O from the environment. In this case, the dinitrosyl formation is exothermic by 0.81/0.91 eV/molecule. This process, being the opposite of the NO adsorption, would involve the same transition state and consequently requires overcoming almost the same energy barrier.

A lower energy barrier, with almost the same energy gain, is possible when a gas-phase NO molecule binds to an already adsorbed one (last reaction of Table III). The energy barrier for this case has to be lower than in the previous one, since this process involves no breaking of bonds, while the terminal oxygens of MoO_3 surrounding the adsorbed NO will attract the N atom of the gas-phase NO. The calculated lowest energy, together with the expected low barrier, support the presumption that this is the dominant dinitrosyl formation mechanism.

Combining the previous results, the proposed mechanism for the reduction of NO is described in the following series of reactions:



A gas NO molecule is exchanged with a $MoO_3(010)$ terminal O, and the system lowers its energy by 0.03 eV. Alternatively, as mentioned in Section III, a vacancy could be created by the reaction of the surface with some other gas-phase molecule; in that case the products of the reaction would not be necessarily include O_2 . Another

TABLE III: Energetics of the reactions discussed in the text, as calculated in the present work. $\text{MoO}_3(010)[\text{v}]$ refers to a $\text{MoO}_3(010)$ surface with a terminal O vacancy; (g) stands for gas-phase molecule and (a) for adsorbed molecule. The energies for the reactions involving adsorbed dinitrosyl are the averages of the two considered configurations mentioned in Section IV.

Vacancy formation:	
$\text{MoO}_3(010)$	$\rightarrow \text{MoO}_3(010)[\text{v}] + \frac{1}{2}\text{O}_2(\text{g})$ -2.95 eV
NO adsorption:	
$\text{MoO}_3(010)[\text{v}] + \text{NO}(\text{g})$	$\rightarrow [\text{MoO}_3(010)[\text{v}] + \text{NO}(\text{a})] + \frac{1}{2}\text{O}_2(\text{g})$ +2.98 eV
$\text{MoO}_3(010) + \text{NO}(\text{g})$	$\rightarrow [\text{MoO}_3(010)[\text{v}] + \text{NO}(\text{a})] + \frac{1}{2}\text{O}_2(\text{g})$ +0.03 eV
(NO) ₂ adsorption:	
$\text{MoO}_3(010)[\text{v}] + 2\text{NO}(\text{g})$	$\rightarrow [\text{MoO}_3(010)[\text{v}] + (\text{NO})_2(\text{a})] + 3.85$ eV
$\text{MoO}_3(010) + 2\text{NO}(\text{g})$	$\rightarrow [\text{MoO}_3(010)[\text{v}] + (\text{NO})_2(\text{a})] + \frac{1}{2}\text{O}_2 + 0.90$ eV
(NO) ₂ formation from adsorbed NO:	
$2[\text{MoO}_3(010)[\text{v}] + \text{NO}(\text{a})]$	$\rightarrow [\text{MoO}_3(010)[\text{v}] + (\text{NO})_2(\text{a})] + \text{MoO}_3(010)[\text{v}]$ -2.09 eV
$2[\text{MoO}_3(010)[\text{v}] + \text{NO}(\text{a})] + \frac{1}{2}\text{O}_2(\text{g})$	$\rightarrow [\text{MoO}_3(010)[\text{v}] + (\text{NO})_2(\text{a})] + \text{MoO}_3(010)$ +0.86 eV
$[\text{MoO}_3(010)[\text{v}] + \text{NO}(\text{a})] + \text{NO}(\text{g})$	$\rightarrow [\text{MoO}_3(010)[\text{v}] + (\text{NO})_2(\text{a})] + 0.87$ eV

NO molecule binds to the already adsorbed one, lowering the energy of the system by about another 0.84 eV. The next step is either desorption of the two O atoms first (as O_2) followed by desorption of the two N atoms (as N_2), or desorption of one O atom first and then of the N_2O molecule. In both cases, an O atom fills the O vacancy that is left behind so that the catalyst is left unchanged at the end of the process. The final state of the system, with N_2 and O_2 molecules is²¹ 1.90 eV lower in energy than the initial state of two NO molecules. The contribution of the catalyst in the process is twofold: first, it can reduce the barrier for NO reduction, and second, it makes it much more probable for two NO atoms to come close to

each other and react.

Acknowledgments

I.R is grateful to Dr. Leeor Kronik for valuable advice regarding high-performance Broyden mixing algorithms, and to Dr. Umesh Waghmare for stimulating discussions. This work was supported in part by Harvard's Materials Research Science and Engineering Center, which is funded by the National Science Foundation.

¹ I. Halasz and A. Brenner, *Appl. Catal. B* **2**, 131 (1993).
² H. C. Yao, *Appl. Surf. Sci.* **19**, 398 (1984).
³ K. T. Queeney and C. M. Friend, *J. Chem. Phys.* **107**, 6432 (1997).
⁴ K. T. Queeney and C. M. Friend, *Surf. Sci. Lett.* **414**, L957 (1998).
⁵ N. Wooster, *Nature* **127**, 93 (1931).
⁶ R. W. G. Wyckoff, *Crystal structures*, 2nd ed. (Interscience Publishers, New York, 1963).
⁷ M. Chen, U. V. Waghmare, C. M. Friend, and E. Kaxiras, *J. Chem. Phys.* **109**, 6854 (1998).
⁸ X. Yin, H. Han, and A. Miyamoto, *J. Mol. Model.* **7**, 207 (2001).
⁹ L. Kihlborg, *Ark. Kemi* **21**, 357 (1963).
¹⁰ N. A. Modine, G. Zumbach, and E. Kaxiras, *Phys. Rev. B* **55**, 10289 (1997).
¹¹ P. Hohenberg and W. Kohn, *Phys. Rev.* **136**, B864 (1964).
¹² W. Kohn and L. J. Sham, *Phys. Rev.* **140**, A1133 (1965).
¹³ N. Troullier and J. L. Martins, *Phys. Rev. B* **43**, 1993 (1991).
¹⁴ L. Kleinman and D. M. Bylander, *Phys. Rev. Lett.* **48**, 1425 (1982).
¹⁵ D. M. Ceperley and B. J. Alder, *Phys. Rev. Lett.* **45**, 566 (1980).
¹⁶ M. Jain, L. Kronik, and J. R. Chelikowsky, to be published (unpublished).
¹⁷ N. Chetty, M. Weinert, T. S. Rahman, and J. W. Davenport, *Phys. Rev. B* **52**, 6313 (1995).
¹⁸ D. Shanno and K.-H. Phua, *Math. Program.* **14**, 149 (1978).
¹⁹ U. V. Waghmare *et al.*, *Comp. Phys. Comm.* **137**, 341 (2001).
²⁰ A. Mihalak, K. Hermann, and M. Witko, *Surf. Sci.* **366**, 323 (1996).
²¹ *Handbook of Chemistry and Physics*, edited by D. R. Lide (CRC Press, Boca Raton, FL, 2000).